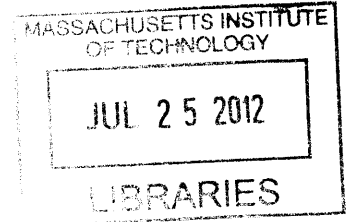# Characterization of Water-Based Liquid Scintillator Response to Gammas and Neutrons at Varying Scintillator-Surfactant Concentrations

by

Lauren Chilton

Submitted to the Department of Nuclear Science and Engineering on in partial fulfillment of the requirement for the degree of:

Bachelor of Science in Nuclear Science and Engineering

at the

MASSACHUSETTS INSTITUTE OF TECHNOLOGY

June 2012

Author's Signature: ____

Lauren Chilton | SB Degree Candidate | DNSE | 11 May 2012

Certified by: _____

Dr. Richard Lanza | Senior Research Scientist | DNSE | Thesis Advisor

Approved by: _____

Dennis Whyte | Professor of NSE | Chairman, NSE Committee for Undergraduates

Characterization of Water-Based Liquid Scintillator Response to Gammas and Neutrons at Varying Scintillator-Surfactant Concentrations

by

Lauren Chilton

Submitted to the Department of Nuclear Science and Engineering on 11 May 2012, in partial fulfillment of the requirements for the degree of:

Bachelor of Science in Nuclear Science and Engineering

Abstract

Large scale solar neutron and neutrino flux experiments require many tons of bulk liquid organic scintillator to take spectroscopic data of these energetic particles. However, material and chemical concerns make such experiments both challenging and costly. In their work, Winn and Raftery prepose a method of water-based scintillator as a viable alternative to liquid organic scintillator. Investigation into the light yield and light attenuation of this material is conducted, providing promising results. The scintillator pair PPO and POPOP serve as the primary and secondary fluor for the bulk scintillator, dissolved in Triton-X surfactant to fix the issue polar/non-polar solubility. A scintillator mixture comprised of 3.000 grams PPO, 0.075 grams POPOP, 240.0 grams of Triton-X diluted in deionized water is identified to produce optimal light yield. The relationship of response of the water-based liquid scintillator to Sodium-22 (^{22}Na) 511 keV gamma source and Americium-24 Beryllium (AmBe) 2-10 MeV neutron source is explored by taking pulse area spectra data at scintillator-surfactant concentrations of 0.5%, 1.0% and 2.0%. An analysis of light yield reveals an increasing linear correlation between observed count rates and increasing scintillator-surfactant concentration. Systematic error inherent in the experiment is discussed and suggestions for future work are proposed.

Thesis Advisor: Richard Lanza
Title: Senior Research Scientist of Nuclear Science and Engineering

Acknowledgments

Contents

List of Figures

List of Tables

1 Introduction

1.1 Motivation

In recent years, organic liquid scintillators have been used in large scale physics experiment investing solar neutron and neutrino fluxes. Large quantities of scintillator are required to see light from energy deposition by these energetic particles. Due to the immense size of the detectors required by such investigations, unloaded or metal loaded organic liquid scintillation has been the optimal choice for large underground apparatuses [Yeh et al., 2007]. Table 1 shows a comparison between these large-scale physics experiments [Bowles et al., 2001, Chen, 2008, Suekane, 2010].

Experiment Name	Location	Scintillator	Chemical	Experiment Cost Est.
Low Energy Neutrino Spectroscopy (LENS)	USA	100 tons	8% In-115	$70 M
High Precision Reactor for Double Chooz	France	200 tons	1% Gd	*unspecified*
Sudbury Neutrino Observatory (SNO+)	Canada	1000 tons	0.1% Nd	$10 M

Table 1: Comparison of Large Scale Neutrino Experiments

Yet significant problems resulting from the use of liquid scintillator have made such experiments both challenging and costly. From the perspective of material demands, these experiments require the preparation of hundreds of tons of sensitive detection material. Scientists must also carefully identify all compatibility issues related to the scintillator composition. Furthermore, the cost of the organic liquid scintillator compounded with immense volume required to achieve the desired energy spectrometry results in significant financial burden.

To alleviate complications associated with organic liquid scintillators at large volumes, Water-based liquid scintillation (W-LS) has been proposed as an alternative. In W-LS, purified H_2O is used as the bulk solution in which a small concentration of scintillator is dissolved [Winn and Raftery, 1985]. Consequently, large quantities of water-based liquid scintillator would be significantly less expensive compared to the same volume of liquid organic scintillator, and compatibility issues with the solution would decrease [Yeh et al., 2007].

Two characteristics are important in defining a successful liquid scintillator: high light yield and long attenuation length. Light yield in a liquid scintillator is a measure of the amount light produced in the scintillator as a function of incident radiation. Organic liquid scintillators boast percent light yields in the range of 30-50%. For W-LS, the percent light yield is much lower (>10% depending on the scintillator concentration) due to the use of water as the bulk solvent [Yeh et al., 2007]. Yet what W-LS lacks in light yield, it makes up for in attenuation length, or distance at which the light traveling through a medium has been attenuated by 63% (1-1/e) [Dai et al., 2008]. Purified liquid scintillators report attenuation lengths of

about 15 m while water-based liquid scintillators can achieve attenuation lengths of 80 to 100 m. A water-based scintillator using a PPO/POPOP fluor pair suspended in a Triton-X surfactant has been proposed by Winn and Raftery as a viable option for large scintillator requirements [Winn and Raftery, 1985].

1.2   Thesis Objectives

The objective of thesis work will be to investigate the light yield of the scintillator proposed by Winn and Raftery with respect to increasing scintillator surfactant concentration. This investigation seeks to produce the following results:

Bulk spectra and coincidence spectra of the scintillator response to radiation sources

A comparison of experimental spectra to predicted particle interaction with the scintillator

Analysis of detector light yield with increasing scintillator-surfactant concentration

1.3   Report Overview

- **Theoretical Background** explains the theory of principles explored during this investigation. Radiation interaction in liquid organic scintillators will be introduced, and details regarding PPO/POPOP scintillator used in this experiment will be provided.

- **Experimental Design** will detail the specifics of the the H_2O apparatus used throughout this investigation, as well as the data collection method required for spectra production.

- **Experimental Methods** outlines the step-by-step process of detector calibration and data collection for investigation.

- **Results** provides the raw spectra collected throughout the experiment and the manipulation of these spectra to produce significant data for comparison. The experimental light yield of this scintillator will be analyzed.

- **Discussion** presents the comparison of spectra data collected within this investigation as well as theoretically expected outcomes. Systematic sources of error and suggestions for future work will be briefly discussed. Finally, a conclusion for this investigation is presented.

2 Theoretical Background

2.1 Radiation in Liquid Organic Scintillator

2.1.1 Overview

The fluorescence process in a liquid organic scintillator is the result of transitions in the energy level structure of scintillator molecules. Absorption of kinetic energy from a radiation particle passing through the scintillator excites the electrons of a molecule from the ground state, S_{00}, to higher energy states (S_1, S_2, S_3, etc.) . For organic scintillators, the energy spacing between S_{00} and $S_{10}$is in the range of 3 or 4 eV, setting the lower bound for the required kinetic energy deposition needed to induce electron excitation. The atom in its excited state consequently seeks to releases this excess energy, resulting in a photon emission. This emission is referred to as "prompt fluorescence" and occurs on the time scale of nanoseconds.
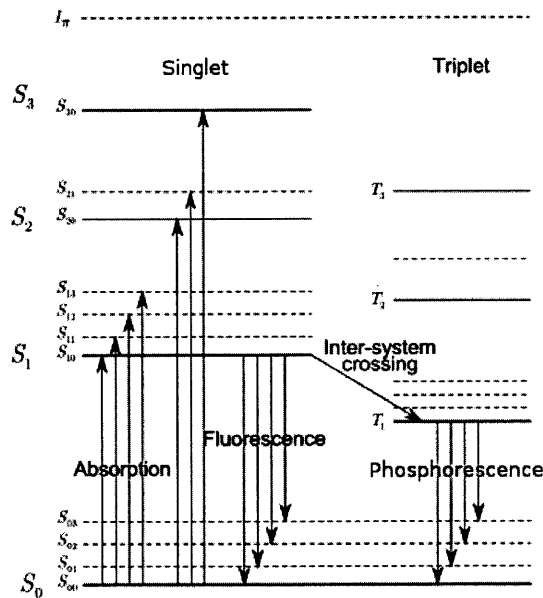
Figure 1: Energy Levels for an Organic Scintillator
adapted from [Knoll, 1979]

Scintillator is transparent to the majority of its own emissions. Figure 1 explains this phenomenon. To excite the electron to the S_1 state, kinetic energy is absorbed by the molecule at a range of energies greater than or equal to the energy level gap between S_{10}. However, the excited atom emits photons at energies lower than the minimum energy requirement for electron excitation, except for the S_{10} to S_{00}emission. This results in minimal energy overlap between the absorption and emissions spectra for organic scintillators, as depicted by 2. The small overlap in absorption and emission spectra represent a range of emitted photon that may be re-absorbed within the scintillator.

In addition to photon emission, organic scintillators feature other de-excitation modes that available
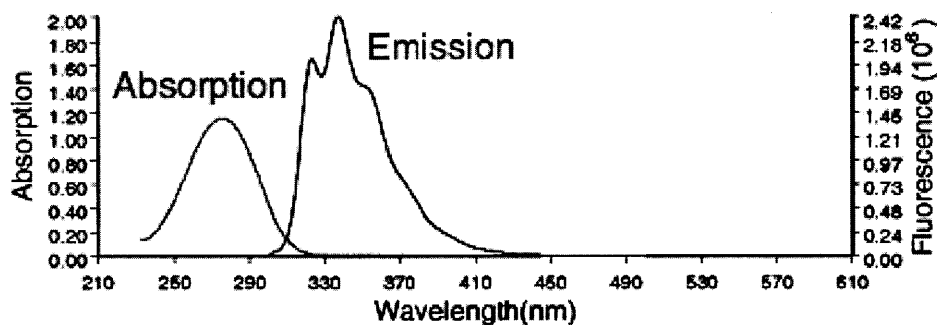
*Figure 2: Sample Absorption and Emission Spectra for an Organic Scintillator
adapted from [Knoll, 1979]*

do not involve light emission. Any de-excitation that does not produce light, either from alternative de-excitation modes or re-absorption by the scintillator, is grouped under the term "quenching". The greater amounts of quenching in a scintillator result in lower scintillation efficiency (fraction of incident radiation energy converted into visible light, of the material).

In addition to the primary fluor, a secondary fluor known as a wavelength shifter may be introduced. The function of the wavelength shifter is to absorb the photons produced by prompt fluorescence from the primary fluor and re-emit that light at longer wavelengths. This interaction minimizes self-absorption in the scintillator and provides a closer match to the spectra sensitivity of a photomultiplier tube. Liquid organic scintillators are produced by dissolving these organic scintillator pairs in an appropriate bulk solvent[Knoll, 1979].

2.1.2 PPO/POPOP Scintillator Pair and Triton-X Surfactant

This investigation focuses on the water-based liquid scintillator proposed by Winn and Raftery. The recipe for this scintillator features water as the bulk solvent with a scintillator pair as solutes. This combination produces a safe and economical bulk scintillator. Table 2 summarizes characteristics of the two scintillators chosen, 2,5-Diphenyloxazole ("PPO") and 1,4-bis(5-phenyloxazol-2-yl) benzene ("POPOP").

Name	Molecular Formula	Absorption Band	Emission Band	Cost [Pla-Dalmau et al., 2001]
PPO	$C_{15}H_{11}NO$	280-340 nm	330-440 nm	$160 per kilogram
POPOP	$C_{24}H_{16}N_2O_2$	200-390 nm	380-460 nm	$1,000 per kilogram

Table 2: Characteristics of PPO/POPOP Scintillator
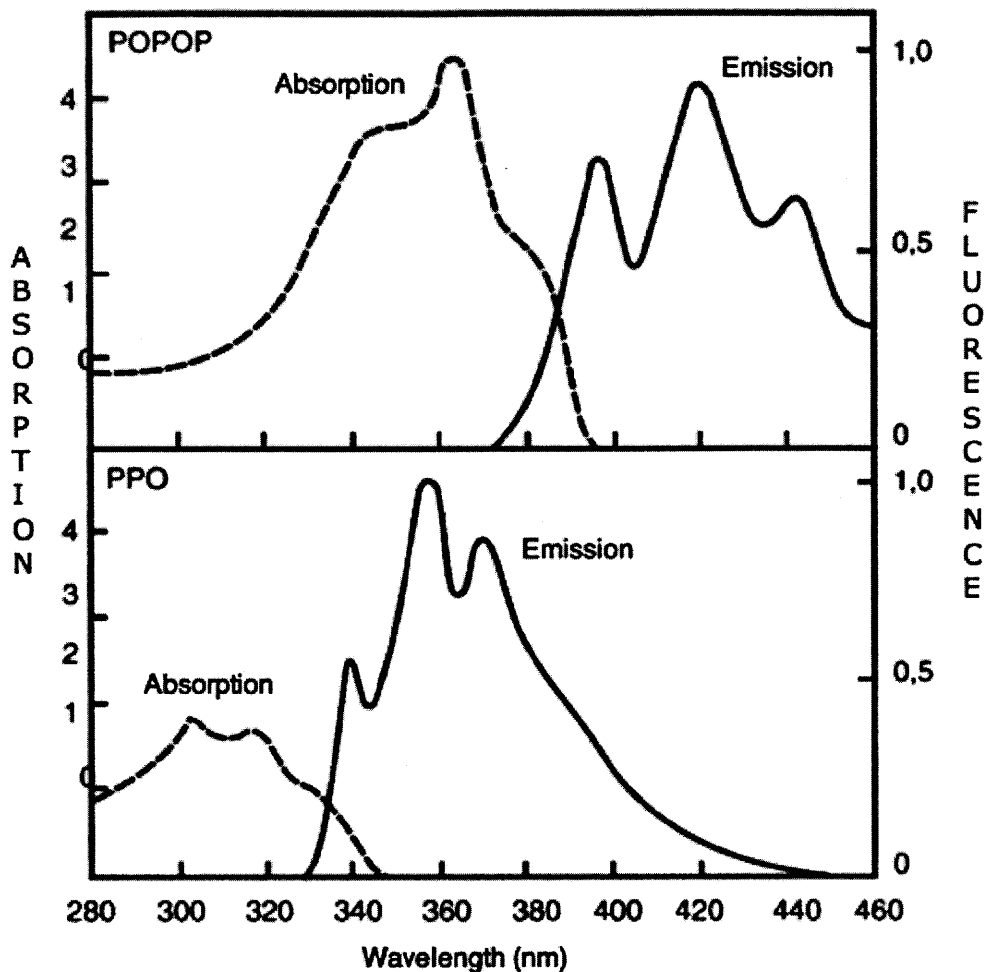
Figure 3: Absorption and Emission Spectra for PPO/POPOP
adapted from Universidad Nacional de la Plata (http://www2.fisica.unlp.edu.ar/~veiga/scintillators.html)

PPO and POPOP were chosen based on their respective absorption and emission spectra, with the absorption band of POPOP (acting as wavelength shifter) closely matching the emission band of PPO (acting as primary fluor). This scintillator pair also features absorption bands far from water absorption bands to reduce the amount of internal quenching in the bulk scintillator. Furthermore, the peak wavelength for light transmission in water is 440 nm, which is well matched to PPO/POPOP emissions. Figure 3 depicts the absorption and emission spectra for PPO and POPOP. The ratio of POPOP:PPO is set at 1:40. This mitigates the expense difference between the two scintillators while maintaing a light yield comparable to a 1:20 ratio.

The PPO and POPOP molecules are both non-polar, making it difficult to dissolve the solutes directly in deionized water (a polar solvent). Thus, Triton-X, a common detergent, is used to help dissolve PPO and POPOP. The tails of the surfactant form a cluster of approximately 50 molecules into which the fluor can

dissolve. Then, the polar heads of the surfactant dissolve into water. Concentrations ranging from 0.5%-3% of the Triton-X, and PPO/POPOP mixture are explored [Winn and Raftery, 1985].

Expected results of light yield with increasing scintillator-surfactant concentrations are depicted in Figure 4. Generally, increasing the scintillator-surfactant concentration of the bulk scintillator results in an increase in count rate for the detector.

Relative Counting Rates for 3 Triton Concentrations vs PPO Concentration
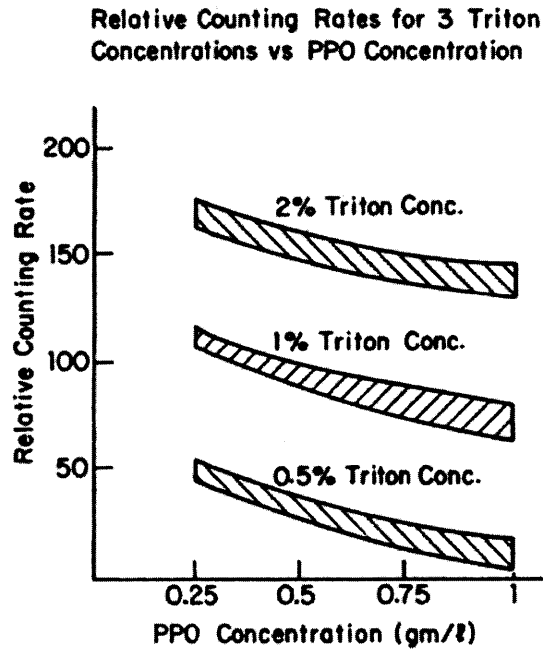
Figure 4: Count Rates for Increasing Scintillator Concentration (Winn and Raftery)

2.2   Radiation Sources

2.2.1   Gamma Source: ^{22}Na

The sodium isotope ^{22}Na undergoes a radioactive decay, emitting a positron with maximum energy 545 keV. The half-life of this isotope is 2.6 years. This positron travels a short distance inside the source, eventually annihilating with an electron. This interaction results in the creation of two photons with energies of 511 keV traveling away from eachother at 180°. Placing a source directly in between two detectors will induce one pulse event in each detector at the same time. A coincidence system can be created in which a pulse detected in one detector opens a data collection window in the other detector. Consequently, the data resulting from a coincidence run should be the result of only the two 511 keV gammas interacting with each detector.

13

2.2.2 Neutron Source: Am-Be

$$^{241}_{95}\text{Am} \longrightarrow {}^{237}_{93}\text{Np} + {}^{4}_{2}\text{He} + \gamma$$
$$^{9}_{4}\text{Be} + {}^{4}_{2}\text{He} \longrightarrow {}^{12}_{6}\text{C} + {}^{1}_{0}\text{n} + \gamma$$
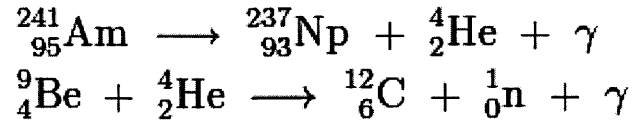
Figure 5: Americium-241 Beryllium Decay

Figure 5 shows the decay process by which the Americium-241 and Beryllium interact to produce neutrons. Americium-241 decays to Neptunium-237 with a half life of 432.2 years, emitting an alpha particle and a gamma ray. The alpha particle then encounters a Beryllium-9 molecule, combining to produce Carbon-12, a neutron, and a gamma. The neutron is emitted at energies in the range of 2-10 MeV. Though the neutron and gamma are not repeatedly emitted in directions exactly 180° opposite eachother, probability dictates that neutrons and gammas will sometime be emitted in opposite directions. Applying collimation to either end of this source focuses the resulting gamma and neutron beams, increasing the probability of detecting coincident gamma and neutron events in opposite directions. A coincidence system can be built such that a gamma detector on one end of the source triggers the collection window for the neutron detector at the other end.

2.2.3 Beta Source: Detector Limitations

The investigation the scintillator performed by Winn and Raftery features the response of the detector to ^{90}Sr beta source. A similar source was acquired for this experiment, but a quick calculation of beta attenuation in PVC revealed that the radiation would not be able to traverse the piping material encasing the scintillator. It was then proposed that the ^{90}Sr source be lowered directly into the liquid scintillator through the valve at the top of the apparatus. Unfortunately, the source was too large to fit through the opening. Though it would have been preferable to compare this investigation's detector^{90}Sr response to results received by Winn and Raftery, we did not want to compromise the detector by making modifications allowing for an opening into which the source could be submerged.

3 Experimental Design

3.1 Design Introduction

This section will describe the experimental apparatus and data collection system employed in this investigation. A basic diagram of the full experimental system is depicted in Figure 6. The target of the investigation, a water-based liquid scintillation detector (H_2O detector), was set up to gather bulk spectra data and coincidence spectra data with the NaI detector. The following sections describe the experimental detector in greater detail, as well as the data analysis system implemented in this investigation.
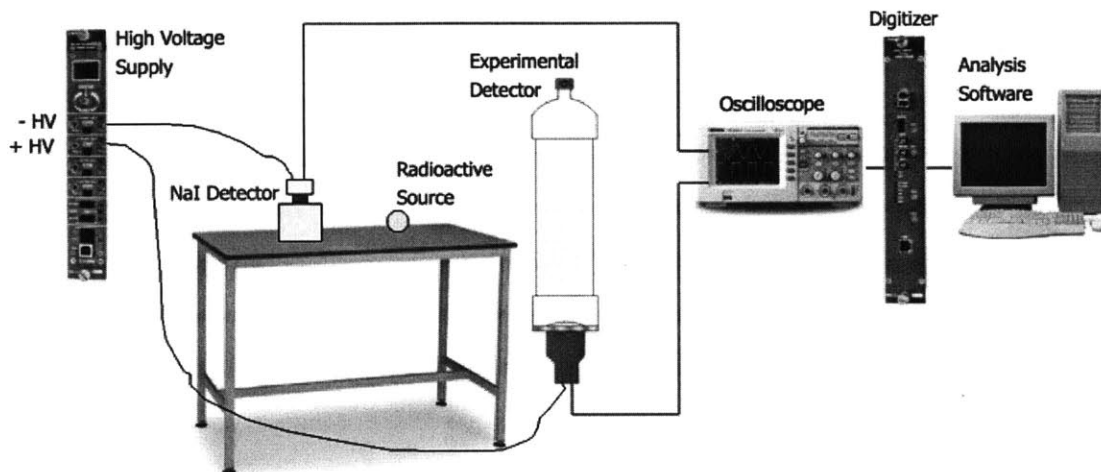
Figure 6: Diagram of Experimental Design

3.2 Apparatus

3.2.1 Detector Design

The H_2O detector design for this investigation is depicted in Figure 7. This "home-made" detector is comprised of a 2' long PVC pipe (6" inner diameter) containing the bulk scintillator. A valve at the top of the apparatus allows the scintillator to be loaded and unloaded with relative ease. A 6"-1" piping junction is fitted on top of the 6" PVC pipe with water-proof glue to couple the two fixtures. A 6" pipe cap is fitted to the bottom of the apparatus with an adjoining metal juncture creating a waterproof seal between the cylinder and a 6" photomultiplier tube (PMT). The apparatus is positioned vertically to allow the lens of the PMT to be in direct contact with the scintillator at all times. The scintillator is contained in a cylinder 2'2" long with 6" diameter. This constitutes a possible scintillator volume of 12.04 liters.

While a range of apparatuses could have been used to house the scintillator, this pre-assembled detector was chosen based on the ease with which scintillator could be loaded and unloaded. To prevent data
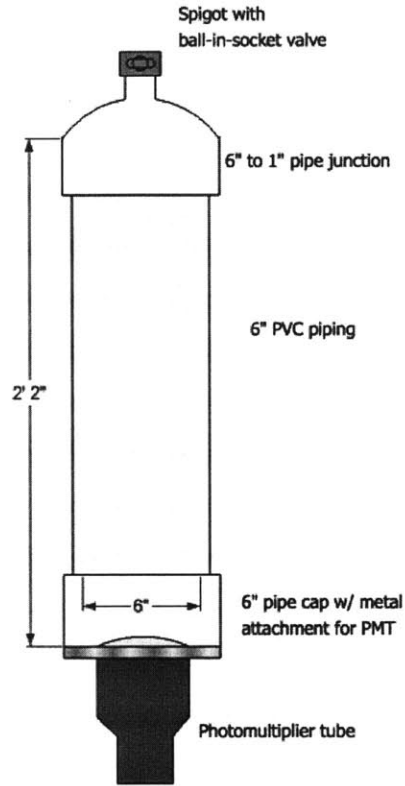
Figure 7: Detector Design Schematic

disruption by light leaks, black tape is wound around the base of the detector and tin foil covers the length of the PVC pipe and valve opening. The detector is situated on a pre-assembled metal frame that lifts the PMT off the ground so two leads (one for the high voltage supply, one for the data collection) may be attached to the base. The fully assembled apparatus can be seen in Figure 8.

3.2.2 Photomultiplier Tube (PMT)

Photomultiplier tubes are detectors sensitive to light produced by radiation in scintillator materials. Photons propagated through the scintillator are focused by the lens of the PMT to a photocathode housed in a vacuum envelope. The incident light initiates the discharge of one photoelectron. The voltage applied to the PMT draws this electron towards the first dynode of a cascade, where some number of secondary electrons are emitted. These electrons are then focused and accelerated to the next dynode, creating more electrons. At the end of the dynode cascade, the gain of the signal is between 10^3 to 10^8. This resulting signal is now large enough to be read by electronic equipment Green [2000].

The PMT used in this experiment is a 6" RCA model with a 14 dynode cascade and a maximum

Figure 8: Picture of Experimental Detector

voltage rating of + 2100 V, resulting in a signal gain of approximately 10^8 Kleinknecht [1998]. This gain amplification makes an auxiliary amplifier unnecessary. Because the PMT is submerged in a liquid composed of mostly water, the bulk scintillator will charge is a negative high voltage is applied. Consequently, a positive high voltage is applied to the PMT keeping the lens at ground. The high voltage is supplied used for this investigation is a Caen NIM module N1470, featuring a 8kV/3mA output range and 4 programmable channels. The operating voltage for the RCA PMT is identified in section 4.1.1 of this document.

3.3 Thallium-Doped Sodium Iodine Detector NaI(Tl)

A Bicron NaI(Tl) detector is required in this investigation to detect coincident gamma events created by the ^{22}Na gamma source and the AmBe neutron source (see sections 2.3.1 and 2.3.2 for an explanation of

17

coincidence detection). This is a popular inorganic scintillator for gamma detection, featuring high light yield and a linear correlation between energy deposited and light created in the material. The detector measures 4"x4"x4" (LxWxH), a smaller volume than the experimental H_2O detector. A voltage of -1700 V is applied to the NaI(Tl) detector by the same Caen module high voltage supply.

3.4 Data Collection

3.4.1 Oscilloscope

The pulses resulting from radiation interaction with the scintillator are viewed on a Tektronix Digital Phosphor Oscilloscope (DPO4045). This oscilloscope is capable of rapidly sampling the pulses produced by the detector to create plots depicting voltage over time (i.e. waveforms) for four different inputs. This specific model is capable of sampling at a rate of 5 giga samples per second (5 GS/s). The oscilloscope also features a manual trigger that applies a threshold to isolate pulses above a certain voltage and register pulse coincidences from multiple inputs. The data from the waveforms displayed by the oscilloscope can be individually selected and saved to a USB drive, however the scope is not capable of performing any analysis on the collected waveforms. Although pulse analysis is not possible, the Tektronix DPO4045 is a useful tool for qualitatively analyzing how the system is functioning (see section 4.2).

3.4.2 Digitizer and Analysis Method

The digitizer used in this investigation is a Caen NIM mod V1720 featuring 8 input channels, 12 bit processing, and sampling at a rate of 250 mega samples per second. Like the oscilloscope, the digitizer is capable of rapidly sampling pulses to produce waveforms depicting voltage versus time. The digitizer then saves these pulses and analyzes the waveform data with respect to either pulse height (the maximum voltage the waveform achieves) or pulse area (the integral of the waveform). A C++ data analysis program is used to call and analyze the data produced by the digitizer.

For this investigation, a specific code was written by Zach Hartwig to analyze the pulses from the digitizer. Figure 9 is a visual representation of how the waveforms are analyzed. A sample window of a few nanoseconds is selected, and an average pulse height is obtained to identify the baseline signal for the pulse. Then, a threshold is applied at a certain height off the baseline such that small fluctuations in the signal are ignored. If a pulse passes through the digitizer with a voltage greater than the threshold, the data from this pulse
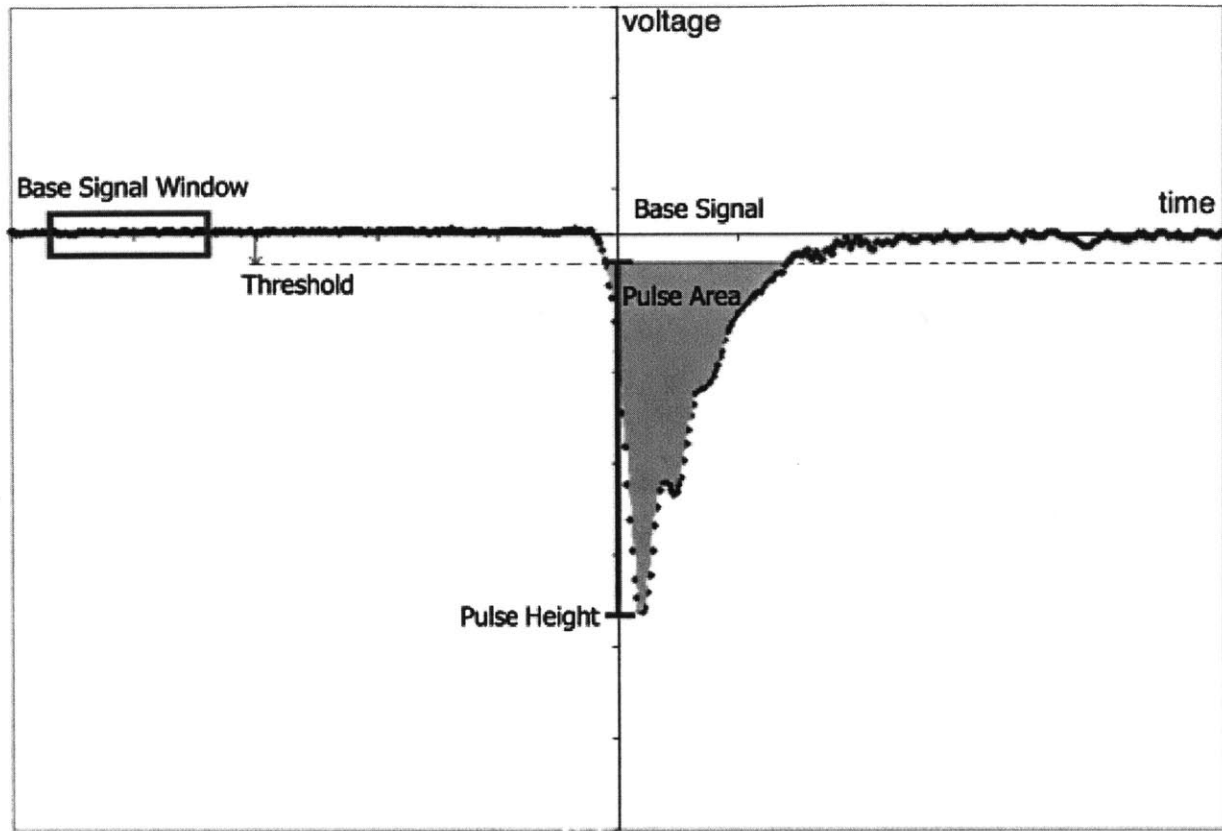
Figure 9: Method of Pulse Analysis

is saved as a waveform. The height and area are then calculated upon completion of data collection, and histograms of the pulse height and pulse area are constructed from the data. These two spectra will depict information about the voltage of measured pulses, and consequently, the energy deposited into the scintillator by the radiation.

4 Experimental Methods

4.1 Pre Data Collection

4.1.1 Initial Apparatus Investigation

Prior to starting the pre data collection, the H_2O detector contained a scintillator with unknown composition and characteristics. In order to confirm that the experimental detector was functioning properly, data was obtained using this unknown mixture to ensure the that there were no obvious light leaks in the system and that the PMT was fully functioning.

After the system was assembled, the oscilloscope was used to qualitatively identify the optimal voltage for the H_2O detector. Scanning the time and amplitude scale, small pulses were observed on a nanosecond timescale as the high voltage supply reached 1500 V. The voltage was slowly raised to 1700V, showing more pulses of various heights. Using the trigger, large pulses were isolated at a rate of roughly two pulses per second. Based on the detector's area and the rate of occurrence, these pulses were assumed to be cosmic rays entering the system. Other pulses registered by the oscilloscope were smaller in magnitude and were most likely the result of other background radiation. The voltage was then slowly raised to + 2100V (the maximum voltage suggested by the PMT) which resulted in too much noise at the base line. Finally, an operating voltage of + 1900 V was chosen for good pulse amplification and low background noise.

To ensure that the detector was operating appropriately, a Cobalt-60 source was placed near the apparatus. This resulted in a higher count rate, with large pulses at the same relative signal height (photopeaks) as well as smaller pulses occurring at a range of lower energies (Compton edge). A pulse height/pulse area spectrum will to confirm this qualitative assessment of detector response to radiation.

4.1.2 Ringing in Signal

Throughout the initial investigation and continuing for the rest of the data collection, a pronounced "ringing" was detected in the background signal. The ringing displayed a specific frequency, appearing in Figure 10, encased in an envelope with its own specific frequency, appearing in Figure 11. The wavelength was calculated for both the ringing and envelope, resulting in $\lambda_{ringing} = 10$ ns and $\lambda_{envelope} = 1$ µs, which correspond to frequencies of $f_{ringing} = 100$ MHz and $f_{envelope} = 1$ MHz. It was determined that the most likely source of this ringing was AM and FM radio signals.
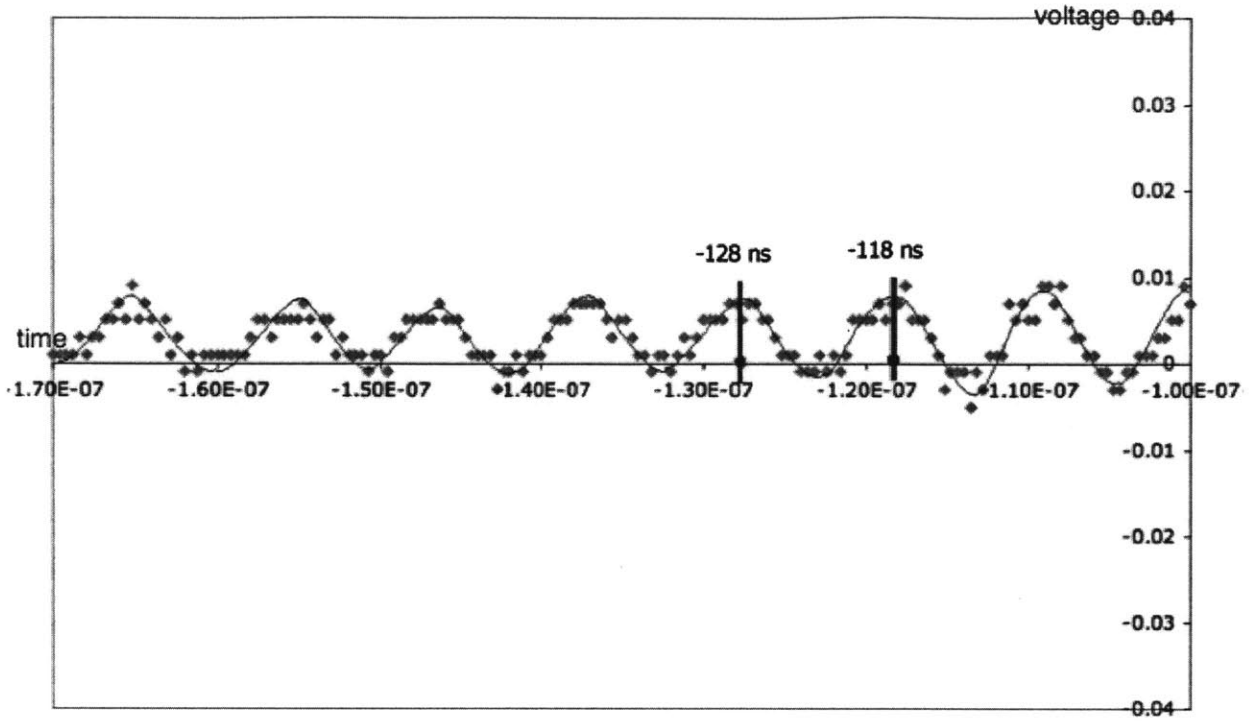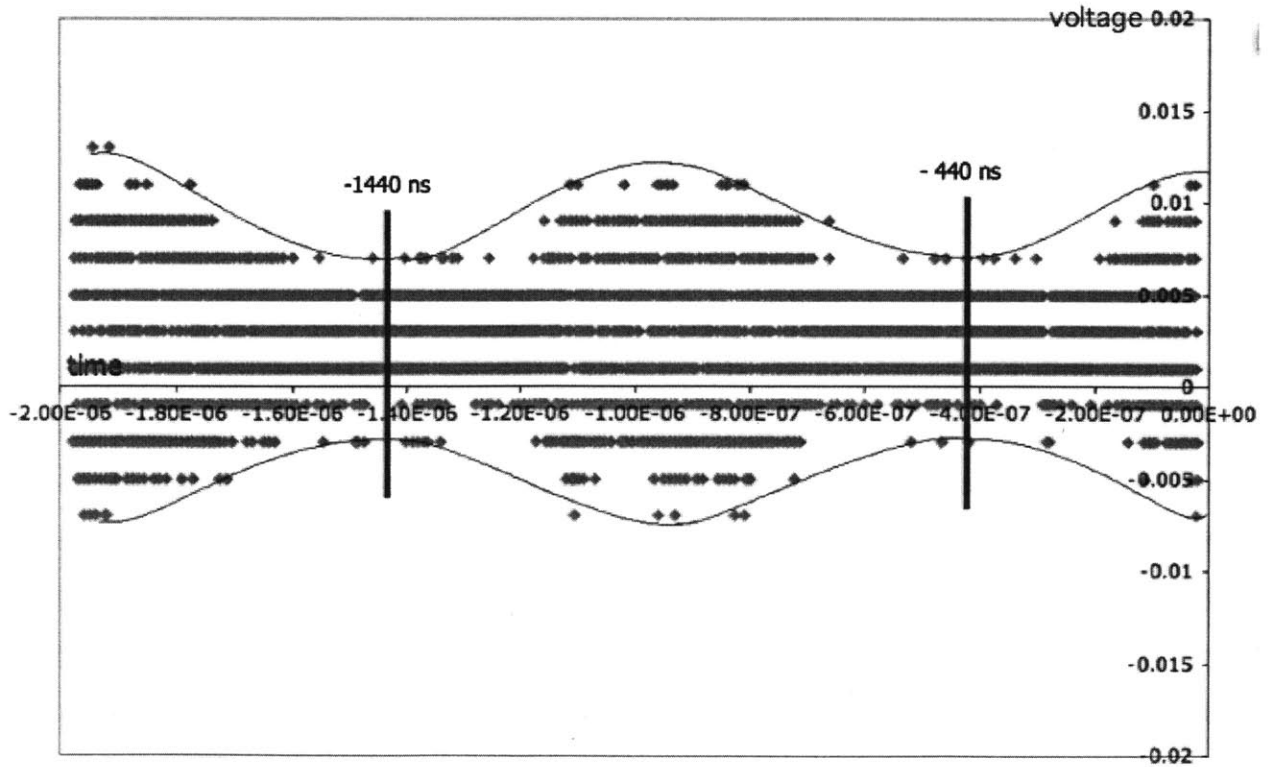
Figure 10: Ringing Sample

Figure 11: Envelope Sample

Depending on the pulse produced by the detector, the interference of the ringing effect in the baseline was found to either produce negligible interference or drastically compromise either the pulse are or pulse height. In Figure 12, the first wave form is the result of a large pulse that saturated the oscilloscope around .77 V, most likely the result of a cosmic ray. Because the pulse size is comparatively much larger than the ringing, the pulse height and area are not compromised. The second waveform is an example of a smaller pulse, most likely due to background radiation. Here, the pulse height seems to be intact, but there are obvious effects of the ringing on the pulse area. Third waveform is another example of a smaller pulse due to background radiation. However, in this example the pulse height is drastically effect by the ringing. Without correction, this will result in inaccurate pulse height analysis.
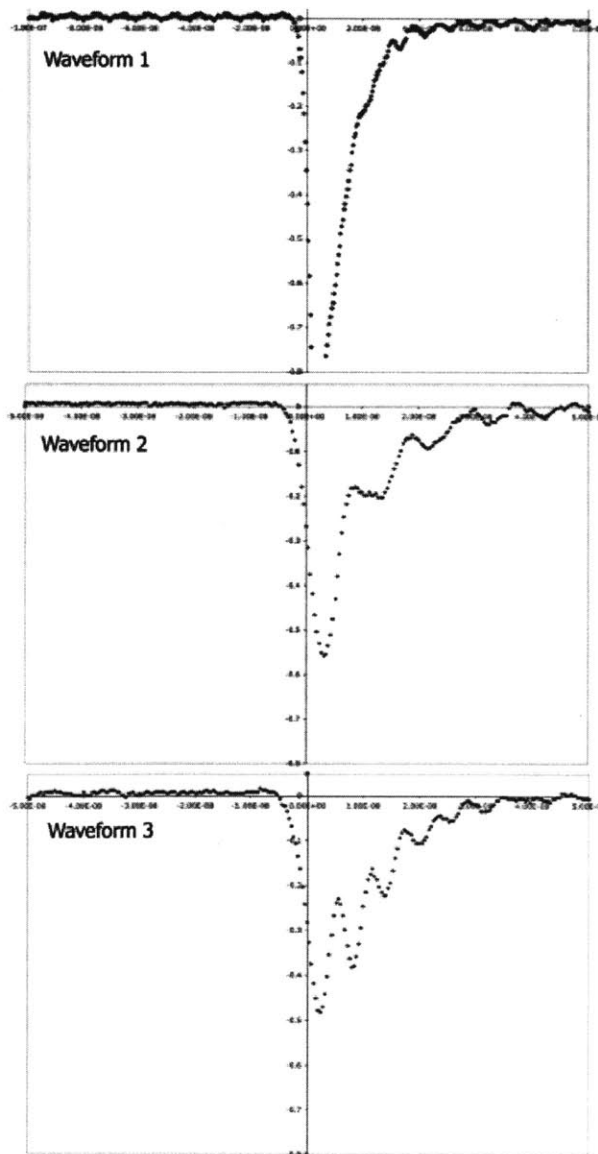
Figure 12: Sample Waveforms

4.1.3 Pulse Heigh Spectra (PHS) versus Pulse Area Spectra (PAS)

A quick investigation was initiated to identify which pulse spectra, height or area, will produce a greater difference between background and source measurement data. First, two background spectra was collected from the H_2O detector for pulse height and pulse area. The detector consistently produced a high pulse rate due to the large size of the scintillator chamber. Even during a background measurement, a run of about 15 minutes produced around 1,000,000 events. Figure 13 shows the two background spectra received when analyzing pulse height or pulse area.
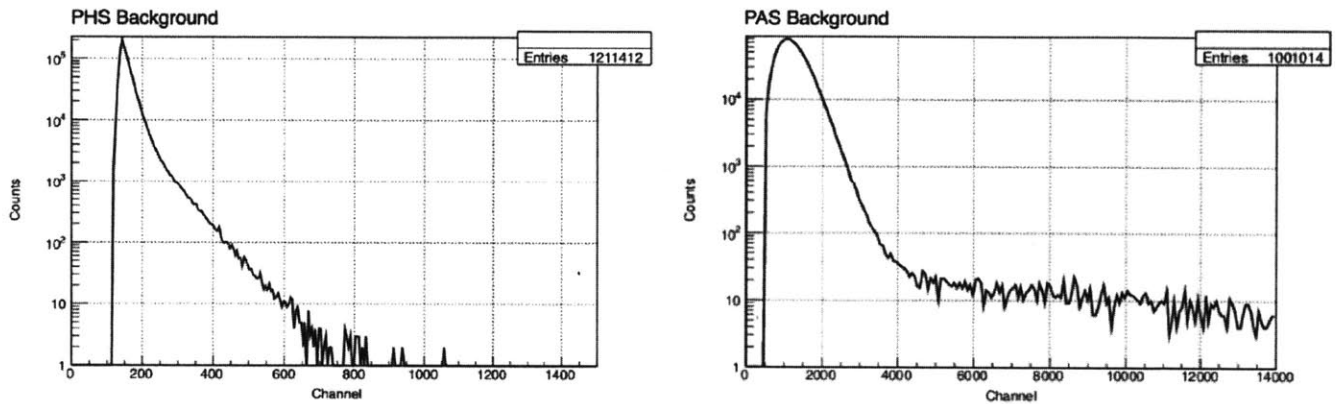

Figure 13: PHS/PAS Background Comparison

The AmBe source was then placed near the bottom of the detector angled upward such that the collimated radiation interacted with a maximal amount of the scintillator. Figure 14 compares the resulting PHS and PAS collected overlaying the previously collected PHS Background and PAS Background.
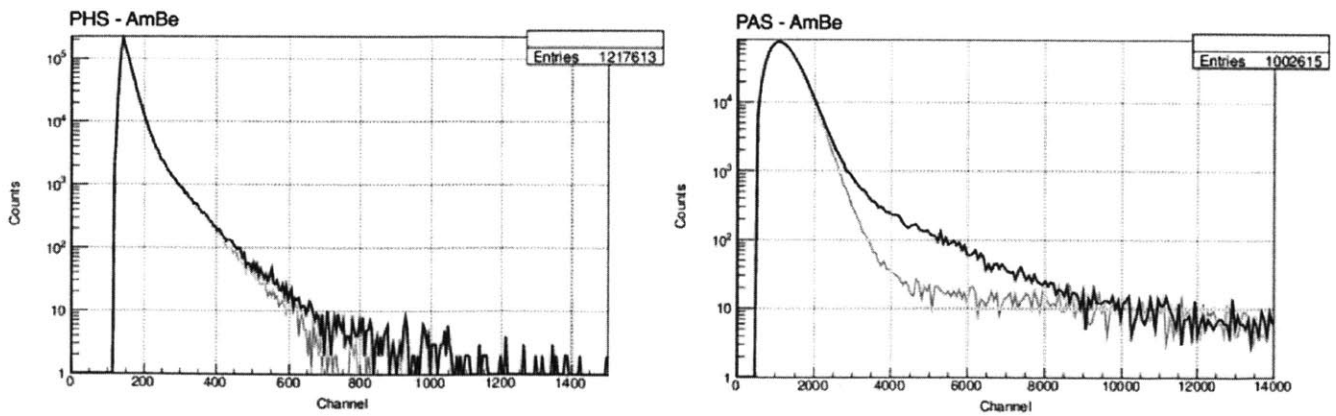

Figure 14: PHS/PAS AmBe Source Comparison

The PHS for the AmBe source shows variation from background in the 500-800 range, however the counts in each channel vary between 2 and 20 counts out of the total 1.2 million counts collected. This indicates that there is little difference in height of pulses resulting from neutron radiation. By comparison, the PAS for the AmBe source shows a distinct departures from the background spectra in the channel range of 2500 to 9000. Here, the counts in each channel vary by one order of magnitude. This consequently implies that there is a large difference between the area of pulses created by neutron radiation and the area of pulses created by background radiation. Therefore, a pulse area spectrum was determined to be superior in providing a distinction between the background data and source data for this detector.

4.1.4 Scintillator Preparation

Before mixing the scintillator, the specific amounts of PPO/POPOP, Triton-X, and deionized water were identified. Given that the detector holds 12.04 L of liquid, calculations were made using 12 L of deionized water as the bulk solvent in which 0.5%, 1.0%, and finally 2.0% of scintillator. An optimal concentration of 0.25 g/l was identified for PPO based on Figure 7 in Winn *and Raftery*. The paper also suggests that little difference in the light yield for ratios of 1:20 and 1:40 of POPOP:PPO. Thus, POPOP concentration in the solvent was set at 0.00625 g/l. The scintillator was then mixed into 240 g of Triton-X (density assumed to be 1) to reach 2% scintillator-surfactant concentration in 12 L. The final mixture requirements for the experiment are outlined in Table3.

	Mixture Requirements	Experimental Values	Error
PPO	3.000 grams	3.0916	± 0.00005 grams
POPOP	0.075 grams	0.0768	± 0.00005 grams
Triton-X	240.0 grams	250 grams	± 5 grams
DI H_2O	12 L	12 L	± 0.5 L

Table 3: Experimental Scintillator Mixture

A properly ventilated chemical lab was used to mix and measure the scintillator. The PPO and POPOP powder were measured on a digital scale and then mixed together at the bottom of a 500 mL glass beaker. Triton-X was then poured in over the scintillator powder. The viscous material was gently mixed and then left to sit for a few days to allow complete *emulsion* of the scintillator.

After the initial investigation of detector (see section 4.2.1), the detector was unloaded, cleaned, and reloaded with 12 L of deionized water. 60 grams of the scintillator-surfactant mixture were loaded into the detector to achieve the desired 0.5% concentration. Once all the data was collected for this concentration, 60 grams more of scintillator were loaded into the detector to reach 1.0% scintillator-surfactant concentration. More test were conducted, and the final 120 grams of scintillator were loaded to reach 2.0%.

4.2 Detector Response Investigation

4.2.1 Bulk Spectra Measurements with ^{22}Na and Am-Be Source

The objective of the bulk spectra measurements are to collect background and source data for a certain number of total counts. This method of max count collection is used instead of data collection with a set time because the bulk spectra will ultimately be normalized to an area of 1 and proportionally compared, making the exact timing of the data run superfluous.

Beginning at 0.5% scintillator-surfactant concentration, a bulk background spectrum was taken from the H_2O detector operating at 1900 V. Next, a collimated ^{22}Na source was placed on a table 10" away from the detector surface, and a bulk spectra was collected until a similar count rate was achieved. Finally, the AmBe source was positioned on the table as close to the detector as possible (approximately 1" away) with the horizontally collimated neutron beam perpendicular to the central vertical axis of the H_2O. Spectra was again collected for a specific number of counts. After collecting the coincidence spectra at 0.5%, the scintillator-surfactant concentration was raised to 1.0% then ultimately 2.0%, repeating the same three spectra measurements. This resulted in a total of 9 sets of bulk pulse area spectra collected from the H_2O (3 background, 3 with^{22}Na, and 3 with AmBe).

4.2.2 Coincidence Spectra Measurements with ^{22}Na and Am-Be Source

The objective of the coincidence spectra measurements are to collect background and source data only occurring when both the H_2O and NaI(Tl) detectors registered pulses. It is imperative for each data set to be collected for the same amount of time so the coincidence event rates could be compared without any ambiguity. Due to the need for coincidence to register an event, the count rates throughout these spectra are much lower than those seen in the bulk spectra measurement, consequently requiring a much longer run time .

After the 3 bulk spectra measurements were collected at 0.5% scintillator surfactant concentration, the NaI(Tl) detector was situated 17.7" away from the detector and a coincidence spectra was taken. After 1 hour and 40, it was decided that enough events had been collected for comparison (see section 5.3 for count rate). Then, the ^{22}Na was positioned in between the two detectors, 10" away from the H_2O detector and 7.7" away from the NaI(Tl) detector. These distances are not arbitrary, but rather the result of a calculation to match the solid angle for the source for each detector. Coincidence data was then collected for 1 hour and 40 minutes. Finally the AmBe source was positioned in between the H_2O detector and the NaI(Tl) detector, mimicking the orientation used in the bulk spectra measurements, and coincidence data was collected from the source for 1 hour and 40 minutes. This process was repeated for the two increased scintillator-surfactant

concentrations, resulting in a total of 9 coincidence spectra measurements.

5   Results

5.1   Spectra Measurements

To compare the data collected for varying scintillation concentrations, each bulk spectrum was normalized such that the area under the curve is equal to 1. In doing so, the bulk spectrum displays the percentage of pulse areas instead of definite counts. This analysis allows for comparison across multiple run times and count rates.

Figure 15 depicts the change in the background bulk spectra with various scintillator concentrations. As the scintillator increases from 0.5% to 1.0%, there is an increase in pulses with an area of about 1250 V. However when the scintillator is increased to 2.0%, the percentage of small pulse areas in the range of 500 V to 1000 V greatly increases, consequently reducing the proportion of pulse areas 1000 V and higher.
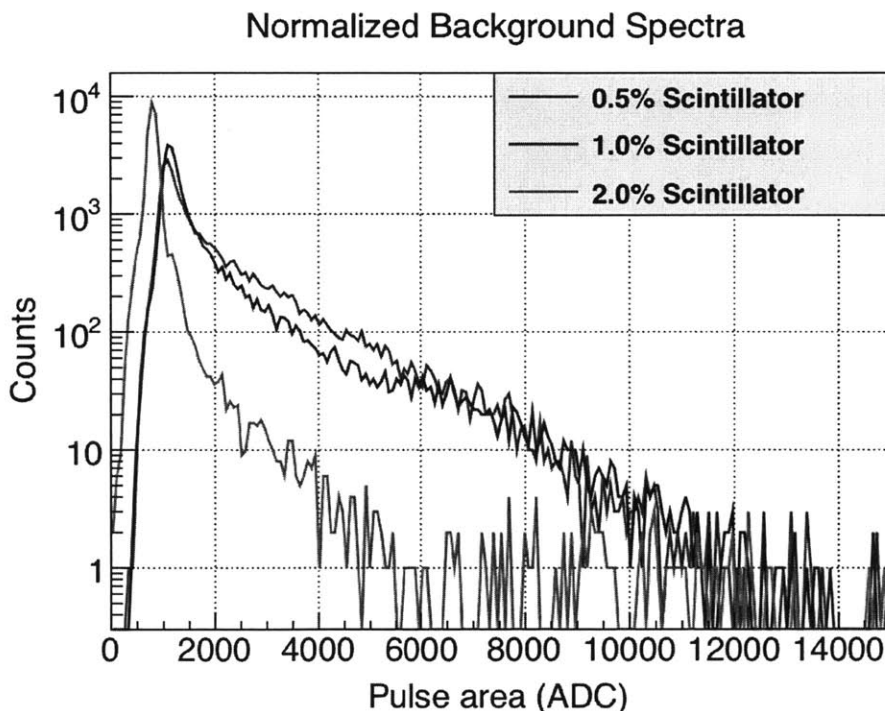

Figure 15: Normalized Bulk Background Spectra (0.5%, 1.0%, 2.0%)

Figure 16 shows the progression of the pulse area spectra response by the detector to 511 keV gammas from the ^{22}Na source. At 0.5% scintillator concentration, the introduction of the gamma source results in a higher percentage of 1000 V pulse areas when compared to the background spectra. Increasing the scintillator concentration to 1.0% results in an increase of 1500 V to 7000 V pulse areas. This increase in pulse area percentages closely mimics the background spectra. The final increase in scintillator concentration to 2.0% continues to increase the percent the range of pulse areas from 1000 V to 10000 V.
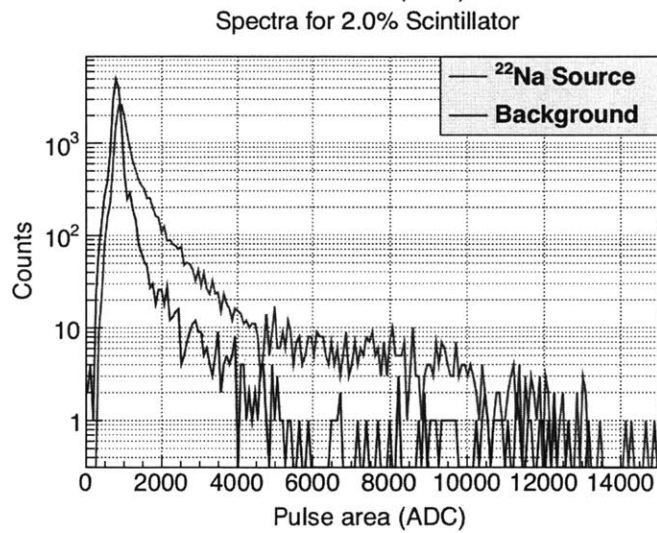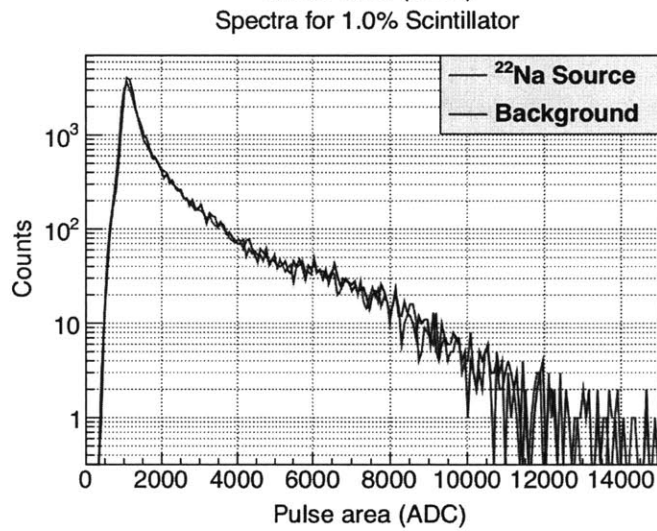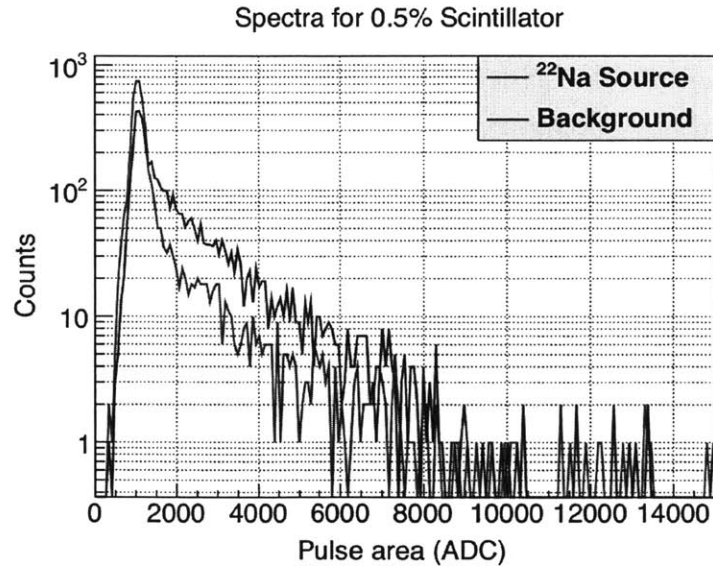
Figure 16: Comparing Bulk Background Spectra to AmBe Spectra (0.5%, 1.0%, 2.0%)
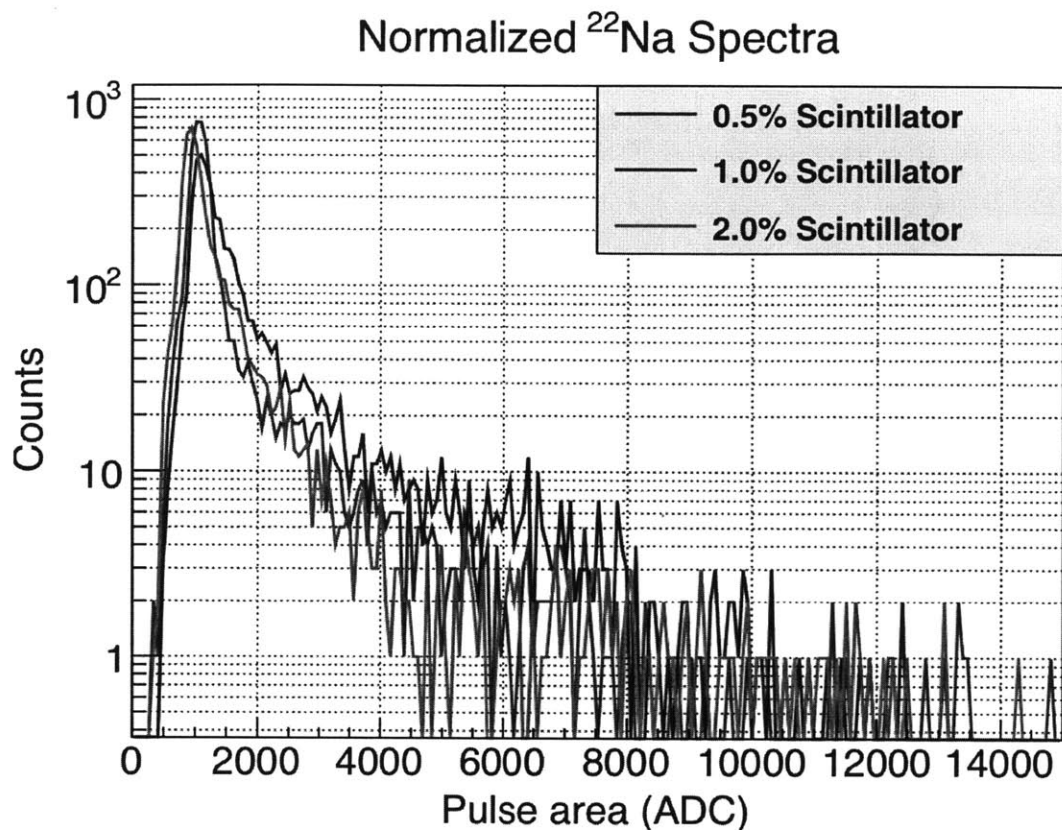
Figure 17: Normalized Bulk Spectra for ^{22}Na Source (0.5%, 1.0%, 2.0%)

A direct comparison of bulk pulse area spectrum resulting from the ^{22}Na source is depicted in Figure 17. No clear trend can be identified with respect to increasing scintillator concentration, though the spectrum shape for each set of data appears to be uniform.

The progression of pulse area detector response to neutrons from an AmBe source is seen in Figure 18. At 0.5% scintillator composition, the greatest percentage of pulse area occurs in the 1000 V to 2000 V range, which is greater than the percentage of background pulse areas occurring at this range. As the scintillator concentration is increased to 2.0%, the percentage of pulse areas with lower energies around 700 V surpasses the percentage of low pulse areas for the background measurement.

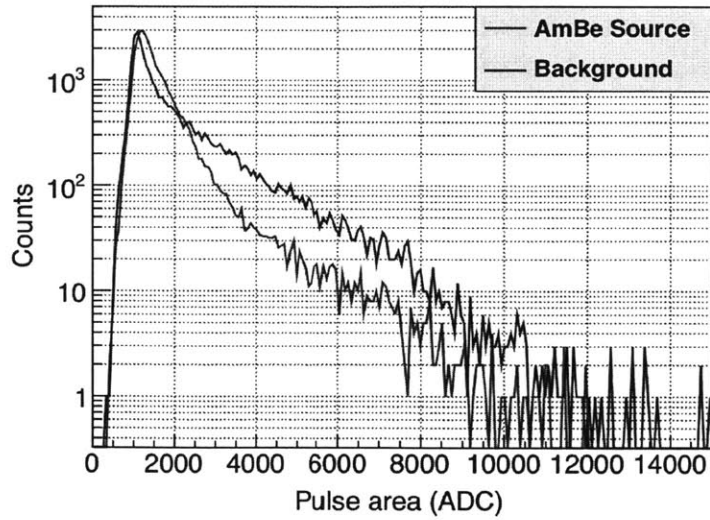Figure 18: Comparing Bulk Background Spectra to AmBe Spectra (0.5%, 1.0%, 2.0%)
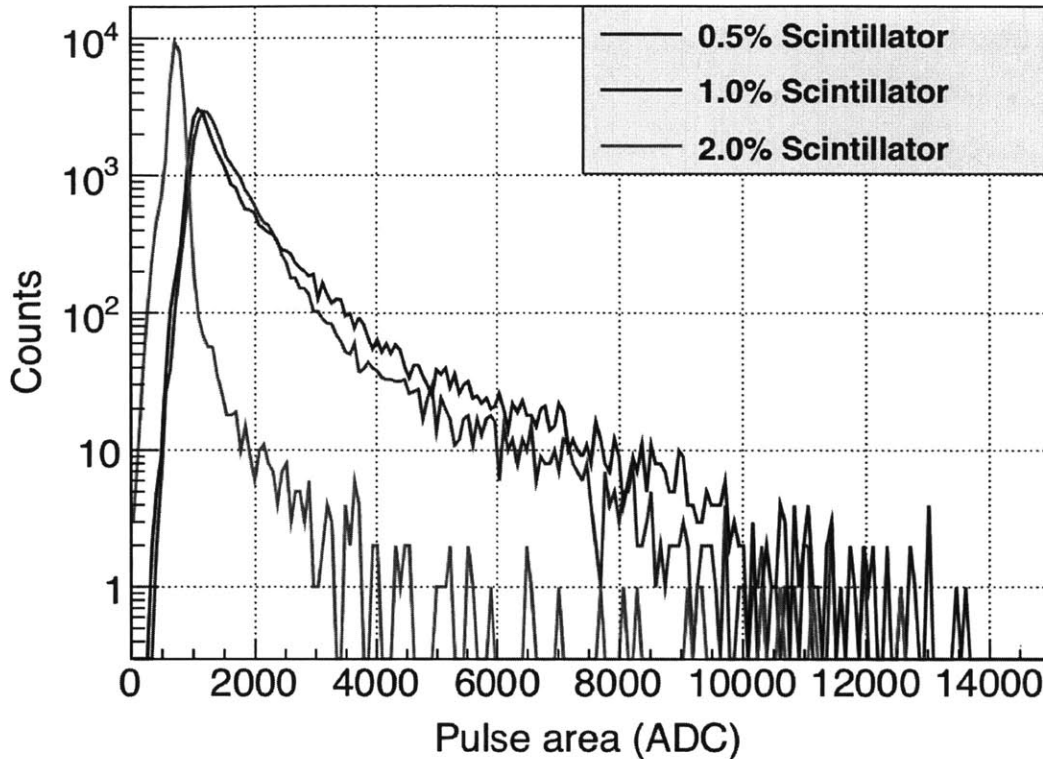
Figure 19: Normalized Bulk Spectra for AmBe Source (0.5%, 1.0%, 2.0%)

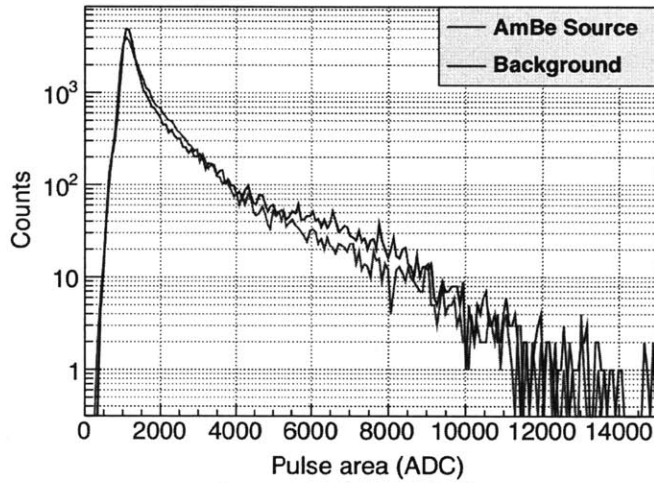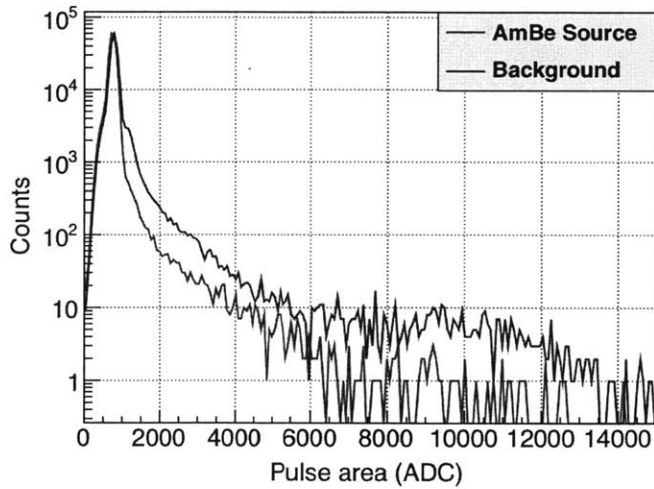When comparing the pulse area response to neutrons from an AmBe source, as shown in Figure 19, it can be inferred that with increasing scintillator concentration, the percentage of pulses with large areas decrease as the percentage of pulses with small areas increase.

5.2 Coincidence Measurements

Figure 20 depicts the results from H_2O detector data taken in coincidence with NaI(Tl) detector when exposed to the ^{22}Na gamma source. The first figure shows the pulse area coincidence spectra received from the detector, while the second figure shows the background subtracted response. Subtracting the background from the data results in a more narrow peak, removing most counts with pulse areas 2000 V and higher. The background-subtracted spectrum's maximum peak height and peak average both occur at approximately 1250 V.

Figure 21 depicts the results from H_2O detector data taken in coincidence with NaI(Tl) detector when exposed to the AmBe neutron source. The first figure shows the pulse area coincidence spectra received from the detector, while the second figure shows the background subtracted. Subtracting the background from

the data results in an overall slight decrease in pulse area counts, however the spectra retains its shape. The background-subtracted spectrum's maximum peak height occurs at approximately 1300 V, while the peak's average occurs at approximately 1750 V.
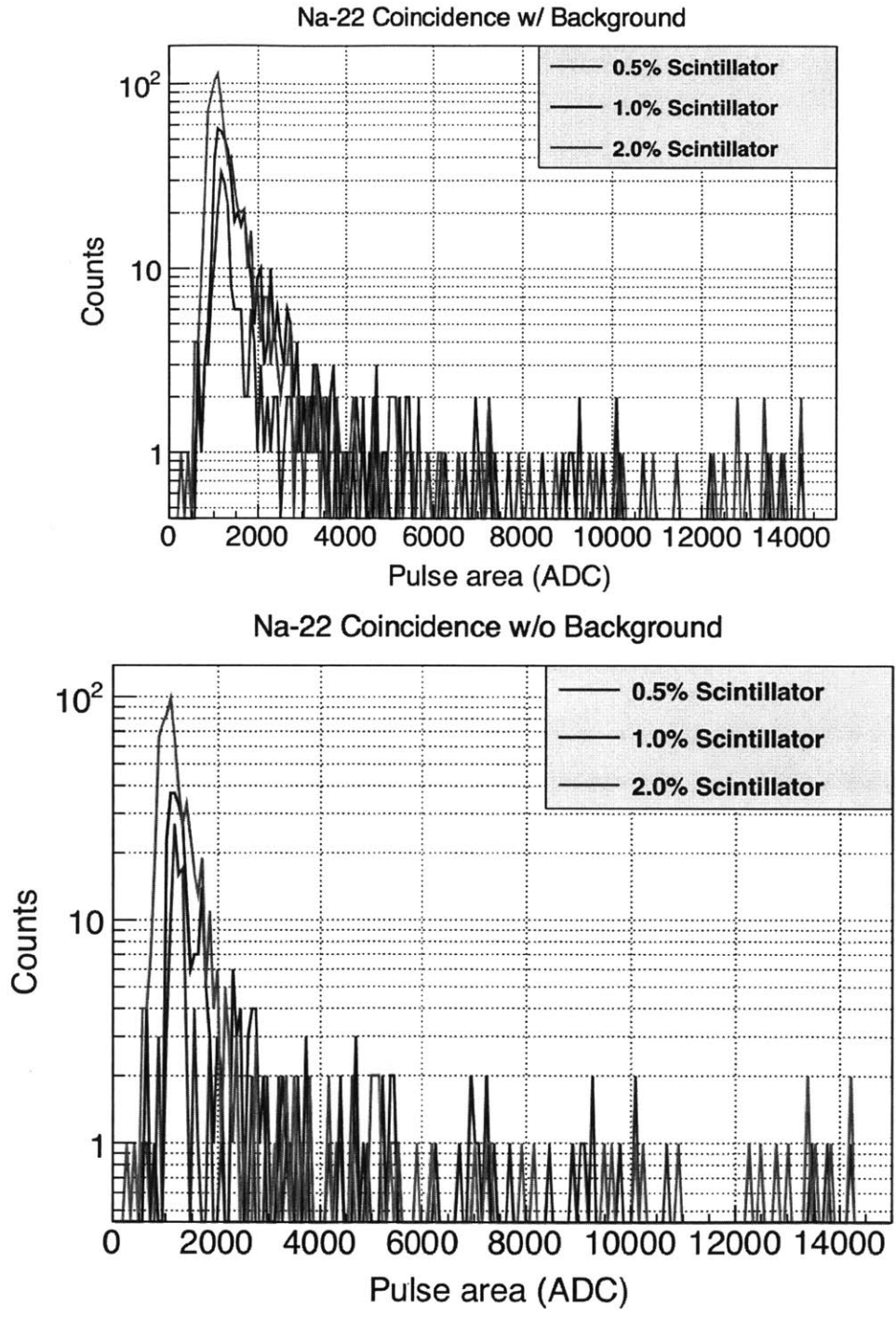
Figure 20: ^{22}Na Coincidence Spectra (0.5%, 1.0%, 2.0%)
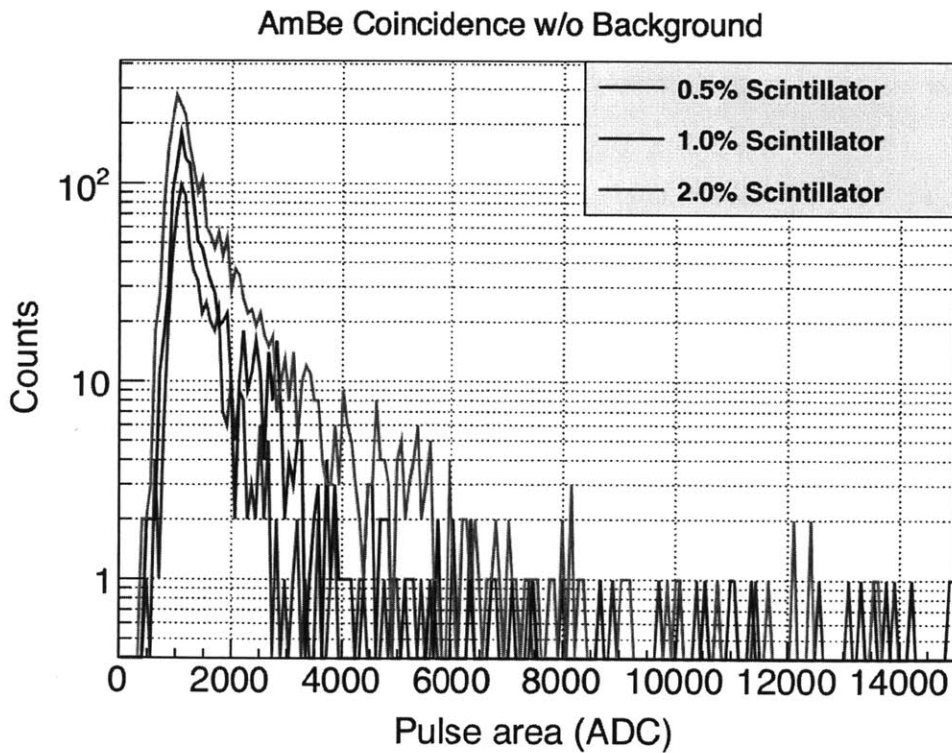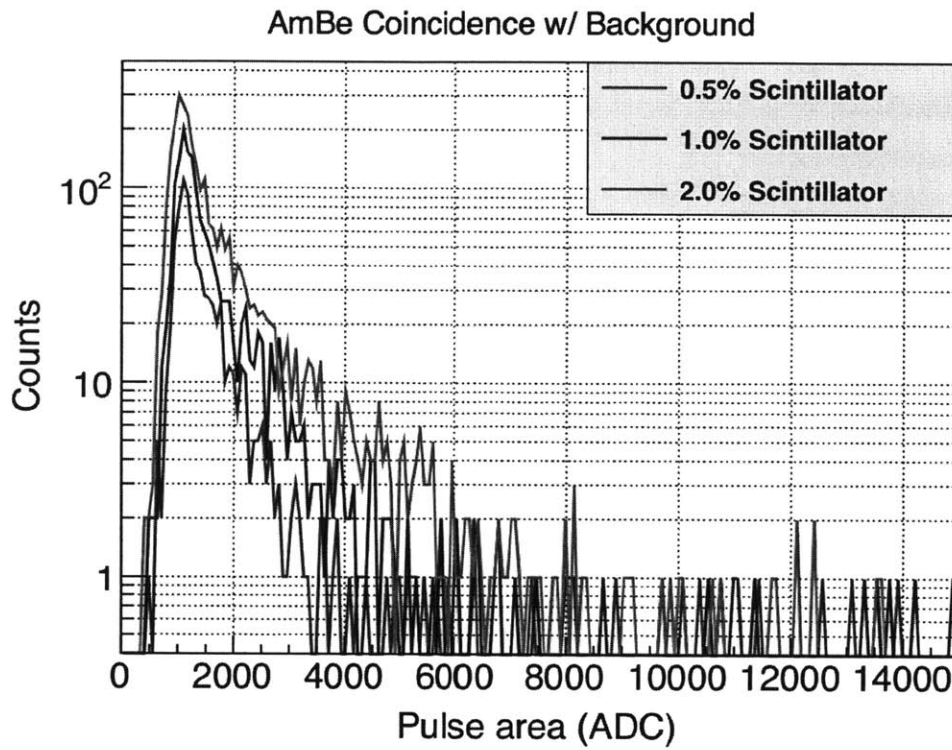
Figure 21: AmBe Coincidence Spectra (0.5%, 1.0%, 2.0%)

The counts collected in each data sample were recorded and placed in Table 4. This data is then graphically expresses in a Figure22. A linear regression is applied to the AmBe, ^{22}Na, and background

Scintillator-Surfactant Concentration (%)	0.5%	1.0%	2.0%
Background Counts	145	307	215
AmBe Source Counts	627	1223	2522
^{22}Na Source Counts	84	228	646

Table 4: Observed Count Rates for Coincidence Data

count data, and the R^2 values are displayed. Both the AmBe and ^{22}Na show a linearly increasing trend with R^2 values greater than .99. By comparison, the data for background counts shows a linear trend at a constant rate, however the R^2 value for this regression is 0.06 indicating an insignificant correlation.
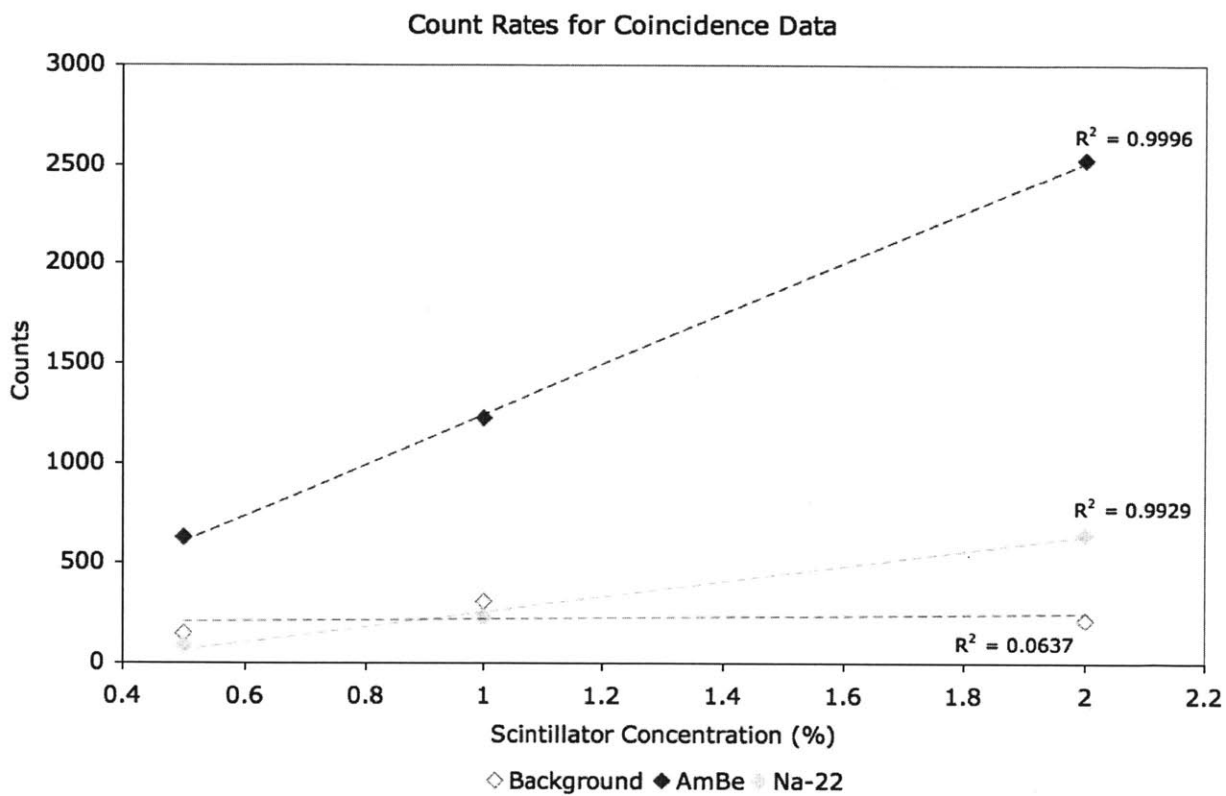
Figure 22: Trend in Coincidence Count Rates for Scintillator

6 Discussion

6.1 Findings

6.1.1 Bulk Pulse Area Spectra Comparison

On a general level of analysis, there are noticeable differences between the spectra collected with ^{22}Na and AmBe and the background spectra. While this suggests that there is some response of the H_2O detector to radiation, it is difficult to discern precisely what these trends indicate. In both the ^{22}Na and AmBe data, the increase in scintillator concentration from 0.5% to 1.0% correlates to an increase in percentage of pulses with smaller areas. This indicates that the PMT registers more low area pulses when exposed to gamma and neutron radiation and consequently more low energy light is produced in the scintillator Unfortunately, the origin of the radiation creating the low energy light cannot be identified with certainty by this spectra comparison. While it would be satisfying to assume that this trend is a direct result from 511 keV gammas and neutrons interacting with the scintillator, other interactions such as background radiation or reflected light within the detector may be the cause.

6.1.2 Coincidence Data and Event Certainty

The coincidence measurements provide a clearer picture of how the H_2O detector responds to the ^{22}Na gamma source and the AmBe. Both Figure 20 and Figure 21 show a high concentration of pulses at lower energies, with average peak energy at approximately 1250 V for ^{22}Na data and 1750 V for AmBe data. Because of the timing required for an event to be in coincidence and the subtracting of a background coincidence spectra, it can be said with certainty that these pulse area spectra are the direct result of 511 keV gammas and neutrons interacting with the detector. For bulk spectra ^{22}Na data, any pulse area greater than 2000 V is concluded to be the result of background radiation, while any pulse area greater than 3500 V in the AmBe bulk spectra data is concluded to be the result of background radiation.

A comparison of coincidence spectra count rates to bulk spectra count rates indicates that while the scintillator is producing large amounts of light, the majority of this light is due to background radiation. For the 2.0% concentration scintillator data, an AmBe coincidence sample time of 100 minutes resulted in 2522 counts, or 0.42 counts/sec. The same scintillator concentration received approximately 1.2 million counts in a sample time of 15 minutes, resulting in a count rate of 1333 counts/sec. Comparing the two count rates shows that 99.97% of all counts received by the detector are due to background radiation.

A qualitative analysis of the shape of the pulse area spectra for both the ^{22}Na and AmBe coincidence data also provides a better understanding of detector response. In both cases, the peak of the pulse area

spectra is at low energies, with higher energy counts occurring with statistically negligible frequencies. However, the ^{22}Na coincidence spectrum features a much more concentrated peak. Furthermore, as the scintillator concentration increases, the pulse shape appears to remain concentrated while the height of the pulse climbs. Because the detector is responding only to gamma rays at exactly 511 keV, an increase in scintillator concentration should increase the occurrence of light at this specific energy rather than increase the energy of light in the detector. The spectra received from the ^{22}Na coincidence data (Figure 20) supports this interaction.

By contrast, the AmBe coincidence spectra features a peak with a sharp rise and a gradual fall. As the scintillator concentration increases, the height of the peak increases and the area of the peak grows leftward towards higher pulse areas registered. In these spectra, the detector is responding to neutrons emitted from the AmBe source with energies ranging from 2-10 MeV. An increase in scintillator concentration will increase the density of the material through which the neutrons are traveling, consequently increasing the amount of energy deposited by neutrons in the scintillator. The deposited energy increase should corresponds to greater pulse area, expanding the pulse area spectra towards the left. Again, the coincidence spectra received from the AmBe coincidence data (Figure 21) supports this interaction.

6.1.3   Concentration Effect on Light Yield

As seen in Figure 22 the number of counts collected by the detector when exposed to radioactive sources increases with increasing scintillator concentration. Furthermore, the number of counts increases linearly with increasing scintillator concentration. This confirms the fundamental knowledge regarding how light is created in scintillators, however it is important to compare this trend to work done by Winn *et al.* in their investigation of this scintillator (Figure 4).The data, depicted in Figure 23, shows count rates higher than this experiment's coincidence data and lower than this experiment's bulk spectra. However, the increase in count rates seems to be slowing to a plateau as scintillator concentration is increased. This differs from the linear trend in counts shown in this investigation.

Relative Count Rates for Increasing Scintillator Concentration
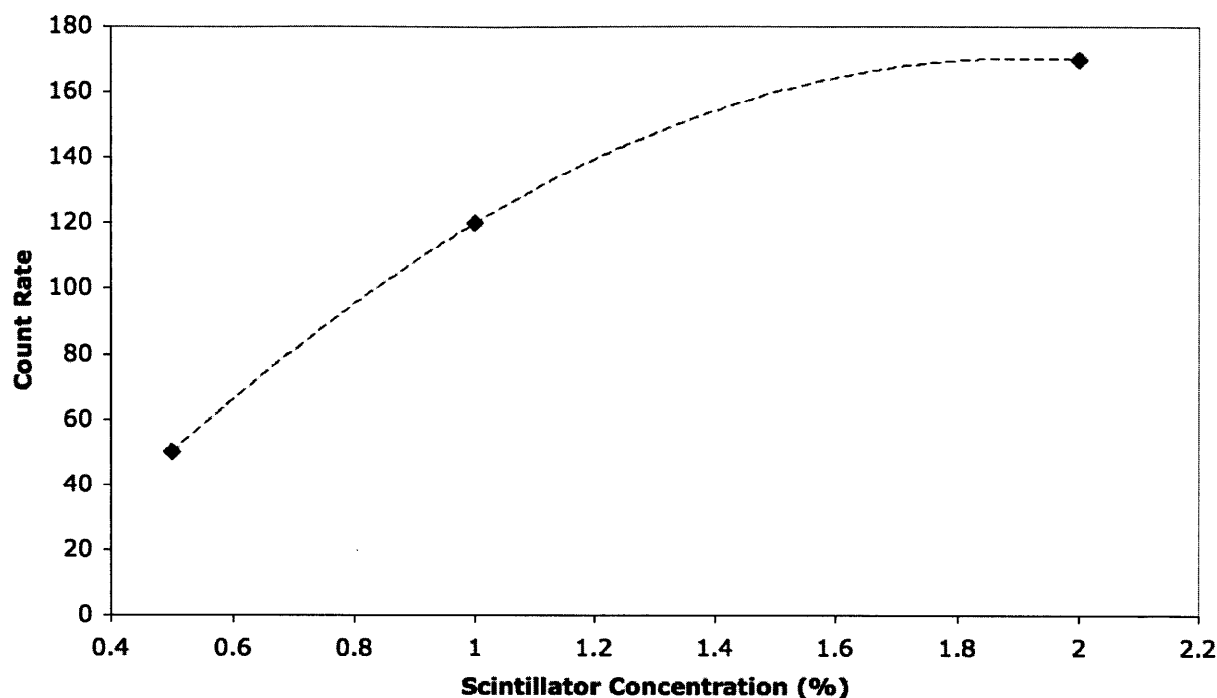**(Winn et al.)**

Figure 23: Count Rates for Scintillator Concentrations (Winn and Raftery)

6.2 Systematic Problems with the Experiment

6.2.1 The Apparatus

The geometry of the detector was not optimal for this analysis. On the most basic level, the sheer volume of the detector allows for greater interaction of background radiation when the data should have been analyzing radiation from the sources. Furthermore, while it can be asserted that the inner geometry of the PVC pipe is cylindrical, the piping junctures lead to uncertainties due to light reflection in the detector. To the investigator's knowledge, there is no focusing of light towards the PMT at the bottom of the tube. Consequently, it would be possible for light to reflect off the walls of the tube many times before reaching the PMT, allowing for noticeable effects of light attenuation.

Ringing frequency effects inherent in the detector also were unaccounted for throughout this investigation. As explained in section 4.2.2 of this document, the ringing sometimes had noticeable effects on the pulse received by the digitizer, creating uncertainty in the pulse height analysis.

6.2.2 Data Collection

For the most part, data collection throughout this investigation was subject to little error. However after the conclusion of experimentation, a realization that the ^{22}Na source was left uncollimated throughout the work. Setting up a simple structure of lead blocks to collimated for the^{22}Na source would have resulted in focusing the two 511 keV gamma rays oriented in opposite directions of each other. This would lead to higher counts for the coincidence data and provide a more complete understanding of the H_2O detector response to 511 keV gammas

6.3 Suggestions for Future Work

While this investigation revealed the response of PPO/POPOP scintillator to background, gamma, and neutron radiation, the scope of is only a narrow sampling of the full characterization for this detector.

One suggested course of future investigation is to tilt the detector onto its side such that the pipe's central axis is horizontal instead of vertical. Orienting the detector horizontally could positively effect many of the unintentional negative aspects of this investigation. In this orientation, placing the collimated source at the end opposite of the PMT would allow for a greater length of radiation interaction with the material while simultaneously reducing the interaction length for cosmic rays. Furthermore, a horizontal orientation would allow for an easy measurement of light attenuation for the scintillator. Data could be taken placing the source at increasing distances away from the PMT, and resulting count rates could be compared to understand the amount of light attenuation in the scintillator material.

6.4 Conclusion

The purpose of this thesis work was to investigate the effects of increasing scintillator-surfactant concentration on pulse area spectra and light yield with in the detector. Bulk pulse area spectra were collected, providing minimal insight into the scintillator's response. A comparison of coincidence pulse area spectra revealed that not only is the detector responding to gamma and neutron radiation sources in different manners, but that these responses appear to correlate to theory regarding gamma and neutron radiation interactions with material. A light yield analysis was performed on the coincidence data revealing a highly linear correlation between scintillator-surfactant concentration and count rate. Though this data differed from results reported of light yield in this scintillator by Winn and Raftery, more knowledge is required of the experimental method for obtaining these results. Overall, this thesis work is the beginning of a promising investigation into the viability of water-based liquid scintillator for large scale spectroscopy experiments.

References

T. Bowles, M. Fowler, A. Hime, G. Miller, A. Pichlmaier, J. Wilhelmy, J. Wouters, J. Bouchez, P. Bourgeois, R. Chipaux, et al. Low energy neutrino spectroscopy. In *APS Meeting Abstracts*, volume 1, 2001.

M.C. Chen. The sno+ experiment. *Arxiv preprint arXiv:0810.3694*, 2008.

X. Dai, E. Rollin, A. Bellerive, C. Hargrove, D. Sinclair, C. Mifflin, and F. Zhang. Wavelength shifters for water cherenkov detectors. *Nuclear Instruments and Methods in Physics Research Section A: Accelerators, Spectrometers, Detectors and Associated Equipment*, 589(2):290–295, 2008.

D. Green. *The physics of particle detectors*, volume 12. Cambridge Univ Pr, 2000.

K. Kleinknecht. *Detectors for particle radiation.* Cambridge Univ Pr, 1998.

G.F. Knoll. Radiation detection and measurement. *New York, John Wiley and Sons, Inc., 1979. 831 p.*, 1, 1979.

A. Pla-Dalmau, A.D. Bross, and K.L. Mellott. Low-cost extruded plastic scintillator. *Nuclear Instruments and Methods in Physics Research Section A: Accelerators, Spectrometers, Detectors and Associated Equipment*, 466(3):482–491, 2001.

F. Suekane. A high precision reactor neutrino detector for the double chooz experiment. *Nuclear Instruments and Methods in Physics Research Section A: Accelerators, Spectrometers, Detectors and Associated Equipment*, 623(1):440–441, 2010.

D.R. Winn and D. Raftery. Water-based scintillators for large-scale liquid calorimetry. *Nuclear Science, IEEE Transactions on*, 32(1):727–732, 1985.

M. Yeh, A. Garnov, and RL Hahn. Gadolinium-loaded liquid scintillator for high-precision measurements of antineutrino oscillations and the mixing angle. *Nuclear Instruments and Methods in Physics Research Section A: Accelerators, Spectrometers, Detectors and Associated Equipment*, 578(1):329–339, 2007.